The mechanics of air entry of drying-cracking soils: Physical models

Boleslaw Mielniczuk, Moulay Saïd El Youssoufi, Tomasz Hueckel

The mechanics of air entry of drying-cracking soils: physical models

Bolesław Mielniczuk[1], *Said Moulay* El-Youssoufi[2], and *Tomasz* Hueckel[1,*],

[1] Duke University, Durham, USA

[2]LMGC UMR 5508, CNRS-Université de Montpellier, France

Abstract. Because of common exposure to high temperatures and forced ventilation of geomaterials in energy production and storage, failure mode of these materials often involves intense drying and constrained shrinkage associated cracking. Previous experiments show that drying-cracking occurs when the materials are completely saturated, practically simultaneously with the onset of air entry and start of desaturation. Computer assisted experiments are presented focusing on the phenomenon of air entry into drying granular meso-scale material models. A critical value of capillary adhesion force is assessed associated with the first (and subsequent) unstable air entries (Haines jumps) into drying capillary water of granular materials, as well as the corresponding saturation. The entries are recognized as precursors of drying cracks. The evaporating models with different separations of grains are photographed every 10 seconds and the images of menisci are computer-processed to follow the evolving water body geometry and cluster saturation. Energy released during subsequent instabilities is also assessed.

.

1 Introduction

One of the many mysteries of soil drying-cracking is that when inspected post-factum it has all the appearance of a highly brittle phenomenon, while it occurs very early in the process in a material that is still completely saturated and certainly ductile (see e.g. Peron et al., 2009). Drying and more generally, penetration of non-wetting fluids into a wetting fluid saturated geomaterial, are phenomena that are relevant to a number of geomechanical and geotechnical technologies of building and transportation infrastructure, conventional and unconventional energy production/management, and many other geo-technologies. These include potential cracking and its prevention in all geologically based barriers subject to heat and ventilation of galleries, liners and buffers in nuclear, industrial and domestic waste disposal, CO_2 injection into a saturated rock, drying of pools of liquid residuals of mineral mining.

The phenomena contributing to drying-cracking are multiple and of uncertain timing, rate, coupling and scale to be represented in. They include evaporation of surficial water, evaporation of capillary and adsorbed clay water, transport

* Corresponding author: hueckel@duke.edu

of water and vapor through the pore and within pore system, air entry, displacement of water/air interface, evolution of suction, suction resultant force and surface tension resultant force, and hence of adhesion force, drying shrinkage, deformation of the pore space/solid skeleton, effective stress evolution due to constrained shrinkage, effect of air entry on stress distribution and stress concentration due to air entry, onset and development of a crack, 1D, 2D and 3D-evolution of drying-crack systems, evolution of permeability in drying crack systems. This is an impressive list of coupled phenomena at diverse scales.

It is essential for security of many energy and infrastructure installations involving wettable materials to predict the conditions for their drying-cracking, monitor for their occurrence, possibly to avoid them through either engineering the service loads, building additional or different barriers, or to invent reinforcement of the barrier materials at any scale, from nano-scale to macro-scale.

Unsaturated soil mechanics (USM) and soil desiccation physics (SDP) is a strange couple, and their marriage is even stranger, if there is any. USM is based on a largely macroscopic, empirical approach, focused on the role of suction alone in affecting the material mechanical strength, and deformability, as saturation varies, due to dewatering/wetting, rarely explicitly addressing drying or any other mechanism. SDP focuses on the value of suction relating it directly to saturation, but often ignores any effect of intergranular forces, and resulting stress in the solid skeleton, or effects of porosity. However, a lot of research, both experimental and numerical, which looks into evaporation from the granular media focuses at a scale of hundreds of grains, Måløy et al., 1992, Jain and Juanes, 2009, Armstrong et al., 2015, Cueto-Fulgueroso and Juanes, 2016. This paper reports experiments at the scale of clusters of a few grains, while interpreting their behavior to help understanding the phenomena observed at the macroscale within the USM framework.

This paper focuses on coupling of some of the multi-physics processes observed at the scale of clusters of several solid grains undergoing drying, and cracking resulting from kinematic constraints imposed externally at a meso-scale. It has been documented that drying cracks in macro-scale experiments form nearly simultaneously with soil attaining shrinkage limit and air entry (Peron et al., 2009a). Shrinkage limit and air entry are phenomenological macro-scale thresholds of water content, or pore pressure commonly linked to averaged variables at the laboratory defined experimental conditions. Here, we focus on the air entry conditions at a smaller scale of grain clusters, which according to our postulate (see Hueckel et al, 2014) constitutes an induced material imperfection, becoming a cause and precursor (in the sense of Scherer, 1992) to an onset of a macroscopic crack propagation of the kinematically constrained drying soil medium.

Computer assisted imagery from experiments is reported, in which a series of several-grain clusters were tested for the configuration of progressing unstable air entries and the associated adhesive force evolution. The tests are designed

to reveal both the dynamics and configuration changes leading to and developing during the air entry events, or liquid/gas interface instability events, known as Haines jumps (Haines, 1930). The adhesive force (see e.g. Orr et al., 1975, Lian et al., 1993, Mielniczuk et al., 2014a, Hueckel et al., 2020) between capillary water and grains at a microscale determines an apparent cohesion of the granular systems at a macroscale. The adhesive force is composed of two components: due to capillary pressure (suction) resultant and surface tension force resultant (Gibbs, 1906; Fisher, 1926). Given than we consider no other forces, in particular solid-solid contact forces, the term intergranular force is used as synonymous with adhesive force. Critical values of the force for a different advancement of the drying process are shown and their dependence on the current saturation for the assemblies with different intergranular space (or porosity).

The current paper is an extension of that by Hueckel et al., 2020. It is based on the same experiments, but its focus and goals are different. The paper investigates new aspects of the drying process and the current results were not published before or discussed. The focus is on the conditions of the instability of the air entry into the capillary water body. The objective is to correlate the onset of such instabilities of the meniscus with the values of the corresponding adhesion force, as well as the relative saturation. First, configurational changes of capillary water body related to the air entry instabilities are presented and discussed for different grain arrangements. Second, a correlation of the onset of such reconfigurations with instabilities of the meniscus and the corresponding adhesion force values, as well as the relative saturation is presented. Finally, energy released during the individual force jumps is assessed. Such energy is believed to be transmitted to deform the solid skeleton and partially dissipate during the process of cracking (Peron et al., 2009b, Holtzman and Juanez, 2010). The meniscus instabilities are precursors of the drying cracking.

USM models link phenomenologically the macroscopic material strength to suction (see e.g. Fredlund et al., 1978 and van Genuchten, 1980) or suction and saturation (Laloui and Nuth, 2010; Alonso et al. 2010). What is known as air entry appears to plays a crucial role in generating such links. However, the physical mechanisms through which possible links arise remain still elusive. Except for two-grain pendular bridges (Gras, 2011; Gras et al., 2013), on the micro-scale, where the phenomenon of the air entry develops, the direct measurement and/or measurement of two principal meniscus curvatures, to deduce local pressure and use it for the air entry criterion, have enjoyed a rather limited success. Thus, postulating a criterion based on a directly measurable advection force, as in this paper, seems to be a step in a promising alternative direction.

2 Experimental background

The experiments discussed below have been in part presented by Hueckel et al. (2020), with the focus on adhesive force evolution. Here, the focus is on the air entry, the first and the successive ones and their effect on the adhesive force. A set of configurational changes of capillary water body related to the air entry instabilities is presented and discussed for different numbers of grains in a cluster and different grain separations,

The apparatus to measure intergranular force and obtain images has the same construction for 3, 4 or 5 grains systems as presented in Fig. 1 (see also Mielniczuk et al., 2014a and Hueckel et al., 2020, for details). It consists of laboratory scale, grain supports and positioning system (XY table and micrometer screw for Z position). As in most of this class of tests they are done with grains being immobilized (mounted on or glued to a rigid support**).** The grain cluster is split horizontally into two parts, with no contact between the upper and the lower part. The upper part consists of 1 grain for 3-grain systems, or 2 grains for 4- and 5-grain systems. The lower part consist of 2 grains for 3- and 4-grain systems, or 3 grains for 5-grain systems. The upper grains are glued to a metal support, which is fixed to a micrometer screw and to the support, without the contact with the scale plate. The lower grains are glued to the support and installed on the laboratory scale. The horizontal distance between grains is fixed, the grains being glued. The lower grains do not move (fixed to scale's plate). The vertical distance between the grain rows is controlled with the micrometer screw, while its horizontal position is adjusted by XY table. Only the upper grains are affected by X, Y and Z adjustments. After the adjustment, XYZ positions are fixed. Then the scale is tared and water is injected between the grains forming a capillary bridge between the grains, and the evaporation test starts. Capillary water between the grains generates adhesive force between grain and water, which actually forms a cohesion between the grains. As a result of evaporation, the reading on the scale changes to negative values (attractive force). This value is interpreted as the intergranular force between the upper and lower rows of grains, which is a uniaxial capillary adhesive force for the cluster, F_{CAP}.

A digital camera has continuously recorded the evolution of the projection of the capillary bridge body during evaporation. To image the moment of rupture, a high-speed digital camera (Vision Research Phantom v12) was employed, with the frame rate of more than 27 000 images per second. The separation between the two sets is set by a micrometric screw. The tests reported in this paper were performed by enabling evaporation at a constant relative humidity in the test chamber of RH=35%, at T=21°C, and at constant separations D (from 100 to 1000μm). The liquid with surface tension of 0.072 N/m is distilled water, the glass beads are precision borosilicate spheres, 3.5 (radius R=1.75mm, 4-grain and 5-grain systems) or 8 mm of diameter (R=4mm, 3-grain systems).

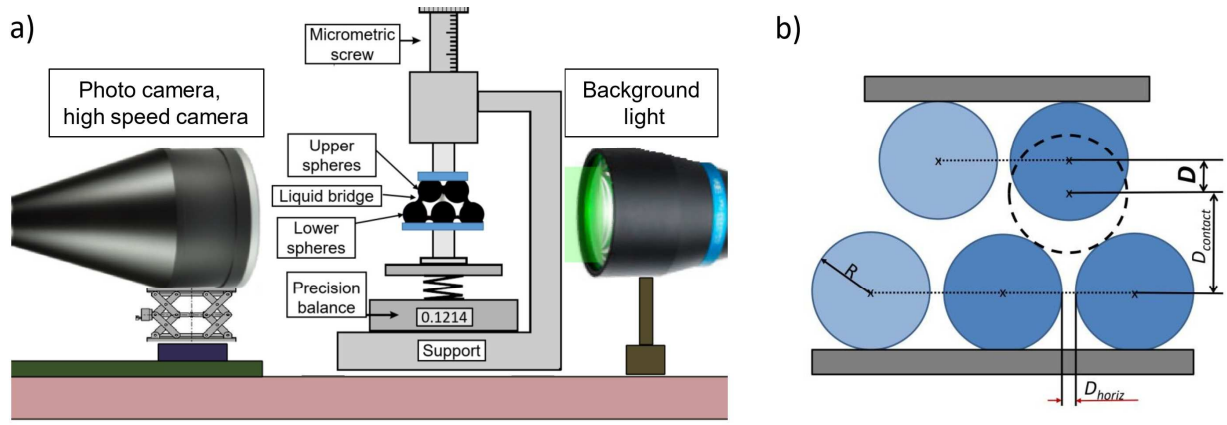

Fig.1 (a) Schematic of the adhesion force apparatus; (b) definition of the vertical *D,* and horizontal, D_{horiz} separations of grains within a 3- or 5-grain cluster

The goal of imaging is to follow the evolution of the wet granular system through the process of drying, by recording the history of the configuration of the gas/liquid interface and simultaneous intergranular force changes, the visible profile interface curvature evolution and whenever possible, the corresponding total capillary adhesive force, - to any degree of approximation - of 5-grain systems, and the 4-grain, 3-grain 2-grain. sub-systems, which evolved from the original ones.

Two types of arrangement of 5-grain clusters have been tested: loose and tight, defined through different horizontal separations between the grains in the top row, and within the bottom row of grains, respectively, 300 and 500 μm for the loose clusters and zero in both rows for the tight ones. The tests constitute an experimental parametric study with respect to the vertical separation D > 0, defined as in Fig. 1b. Notably, direct contacts between the solid grains are not included as an option to avoid a possibility of a silica polymer solid bonding in the terminal phases of drying, when local contact damage might arise (Guo and Hueckel, 2013, 2015).

2.1 Capillary water configuration evolution

Evaporation of monodisperse systems is analyzed at a mesoscale of clusters of a few grains connected by a body of water forming a water bridge, kept in place by capillary forces. Drying of such systems consists of intercalating phases of a relatively slow and relatively uniform phase driven by external evaporation rate (30 minutes), suddenly transitioning into an almost instantaneous (20 sec.) localized air entry phase. The air entry comprises a rearrangement of water mass, with a completely different final interface morphology, followed in most cases, by another phase of slow evaporation-rate controlled process. Interestingly, the modes of air entry occur in three different forms, shown in Fig. 2, consisting in: (i) a thin-sheet instability (Fig. 2a, b and c) – in the case of two-dimensional fragments of the granular

systems, (ii) saddle-form meniscus snap-through (Fig. 2e, f and g) and (iii) formation of a water-wire and its rupture through pinching (Fig. 2d) - in the case of two-grain bridges. A very important aspect of the air entry modes shown in Fig. 2 is that modes (i) and (ii) may develop for systems of any number of grains, except for just two-grain systems, see e.g. Urso et al., 1999. Wire pinching mode (iii) takes place for 2-grains systems, including those formed in the terminal (pendular) phase of larger systems. The latter mode has been discussed in detail by Mielniczuk et al. 2014b, 2015, Lievano et al., 2017, Zhao et al., 2020.

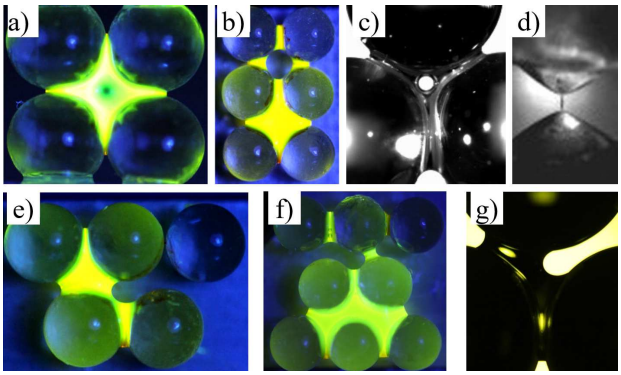

Fig. 2. Examples of three configuration modes of air entry: (a), (b) and (c) - thin-sheet instability for 4-, 6- and 3- grain systems; (d) water-wire formation and a pinch-off for a 2-grain system; (e), (f) and (g) saddle-form meniscus snap-through for 5- 8- and 3- grain systems, respectively.

The above three modes of evolution of the water body configuration depend on the mode of air entry into the water body. The air entry mode is different depending whether it takes place at an air/water interface point of a Gaussian curvature (GC) that is positive (double bowl), negative (or saddle-form meniscus) or zero (flat, at least in one cross-) points. GC is the product of the two principal curvatures of the water body surface. Fig. 3 shows for a 3-grain capillary cluster characteristic points with positive (points 4 and 5) and negative (point 2) GC. For each of these points, radii of principal curvatures are shown in the respective cross sections. When the center of curvature is located within the water body, the curvature is considered positive. The cross section images were reconstructed through X-ray tomography (for details see Hueckel et al., 2013). The images were not obtained along an evaporation process, but via an injection of a prescribed volume of water. In such a body, if an instability would develop at points 2/3, it would be a thin-sheet instability, while at points 4 or 5, it would be a snap through of the meniscus.

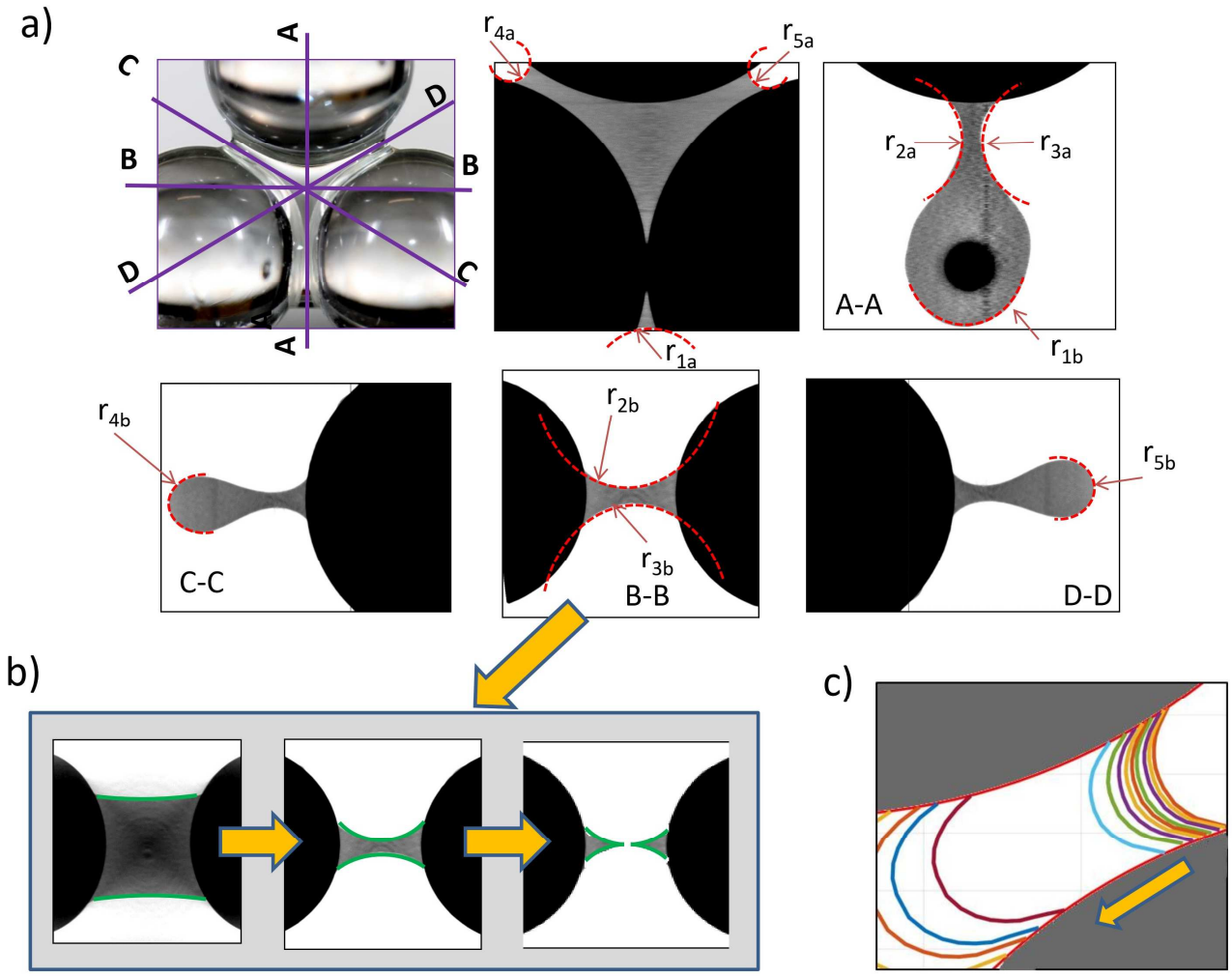

Fig. 3. (a) An image and three cross sections of a configuration of a capillary water bridge between 3 glass grains obtained via x-ray tomography. Gray is water, black is glass, white is air. Curvature principal radii are marked for five different menisci, assumed as circular in their cross sections. The curvature is positive, if the center of inscribed circle is located in water. The configuration shown precedes any instability. Menisci #2 and #3 have a positive Gaussian Curvature. Menisci #1, #4 and #5 have a negative Gaussian Curvature (see Hueckel et al., 2013 for details); (b) schematic of a cross section through thin-film instability at a "double bowl" point as 2/3 above in (a); (c) schematic of a cross section through a saddle-form meniscus snap-through between two positions (shown by an arrow) of equilibrium as in point #5 above in (a).

We perceive the air entry as a local instability of the external water surface (see also Hueckel et al., 2013). The instability for postive GC is in a form of bifurcation of a thin-sheet tension with a void nucleation and spreading, whereas for negative GC, the instability takes a form of a meniscus snap through to a configuration of alternative equilibrium . The evolution occurs in both cases very fast, within about 1/1000 second, which is completely out of time-scale of the evaporation process, hence becoming a fluid dynamics instability phenomenon. More details are presented in Hueckel et al., 2020. Currently, with the imaging techniques employed, we are not able to provide a numerical value of the GC at air entry, nor we are in the position to advance a hypothesis about quantitative criteria for the air entry mode. Further studies are needed to determine the quantitative and physical conditions for the development of these instability modes.

For small clusters of grains, the classical Saturation Degree is not a good measure of the presence of water, mainly because of an ambiguous meaning of pore space volume. Instead, we will use an alternative representation of saturation: Cluster Saturation, CS. Cluster saturation is defined as a ratio between the current total volume of water and the reference total volume of pore space in the initial configuration, equivalent to the initial water volume. The current total volume of water includes water in isolated small capillary water bodies that do not communicate with the "main" body of water contiguous with the stress constrained boundary, as well as water that is attached to the grains via surface tension forces in the "outside" cleft-pore space. This is one possible way to determine saturation varying between 1 and 0 for discrete clusters of different number and arrangement of grains.

In general, the larger the separations, the shorter the time to the first entry and the higher the corresponding critical CS. It is observed that in loose structures (larger grain separations) the air entry events take place through a meniscus instability (at a negative GC point), see Fig. 4, whereas in tighter structures (smaller grain separations) the AE occurs via thin sheet instabilities at positive GC points, see Fig. 5, the left and center column. The localized air entry results into a transition from one configuration to another in an unstable process which involves a fast change in geometry and a rapid displacement of water masses. The patterns of the sequences of air entries depend on the separation.

For largest grain structures of 5-grains investigated in this study, with 3.5 mm grains, it has been seen that the mode of air entry depends on the separations between the grains, which may be seen as a representation of porosity of the macro-scale granular medium. Separation of grains is kept constant over the entire duration of the tests presented, unless mentioned otherwise.

For loose clusters, at the smallest vertical separation of 0.1mm (Fig. 4b, left column), the first air entry occurs at a bottom left meniscus between the two bottom grains. It converts a 5-grain cluster into a non- symmetric system with a pendular doublet and a 4-grain cluster. The subsequent air entry takes place at the right-side bottom meniscus restoring the symmetry, and yields two doublets, and a central top 3-grain cluster. The latter one shares the two top grains with the doublets.

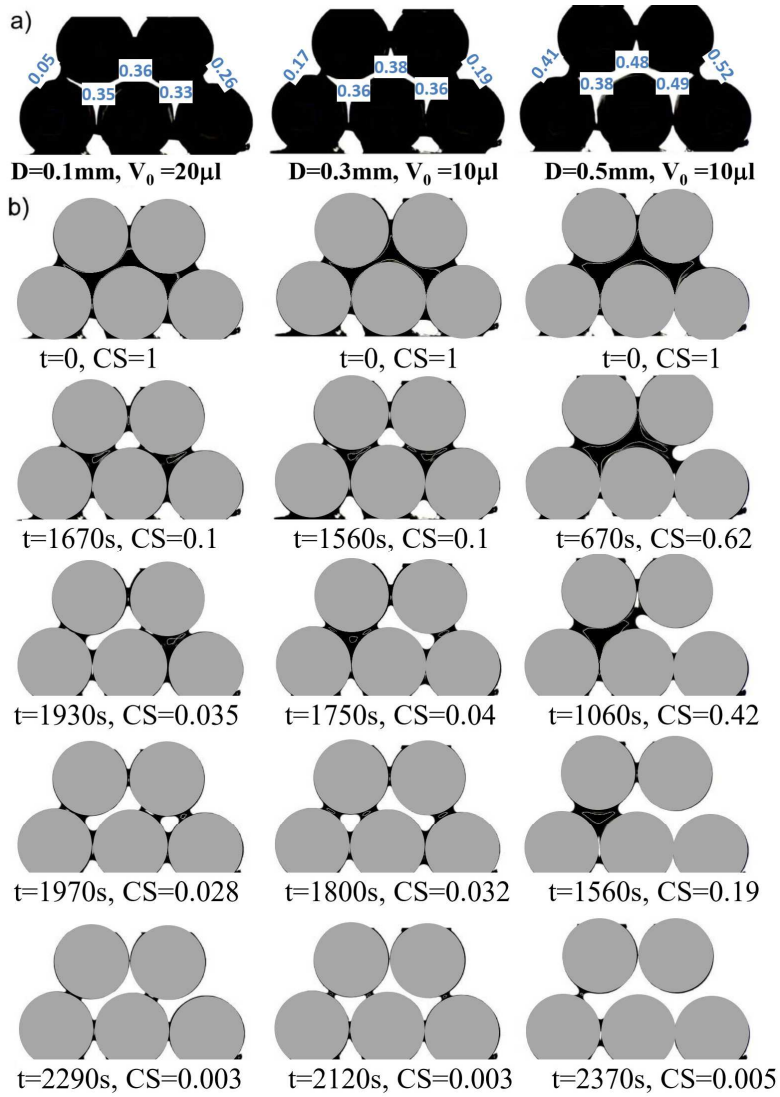

Fig. 4. Loose cluster five-grain capillary water (horizontal projection) transitioning through capillary, funicular and pendular configurations (arranged here in columns from left to right for separations of : D =0.1mm, first column; D = 0.3mm, second column; D = 0.6 mm, third column; D = 1mm, last, fourth column. Horizontal separations in upper row are 0.3 um, in lower row 0.5 um: (a) the outside numbers: the cluster distances between the indicated individual grains, the inside numbers: the initial diameter of a circle inscribed into a pore; (b) changes in capillary water configurations at different Cluster Saturations *S* (from the top to the bottom of the figure) for different vertical separations *D*, column by column.

Further, the side pendular doublets undergo a pinch-off, while the triplet exhibits another air entry via central top meniscus, generating two central doublets. The mechanism of pinch-offs of pendular systems is discussed by Mielniczuk et al., 2015.

Timewise, the first instability occurs at roughly 55% of the time to reach a completely dry state. As discussed by Hueckel et al., 2020, that corresponds to a relatively advanced cluster desaturation, that is after 72% of the initial water volume is gone, at a relatively low cluster saturation of CS = 0.28. Classically, at a saturation degree of the macroscale medium at the air entry is above 0.9. However, the relatively low number for the micro-scale clusters considered here is

not a surprise, as a substantial initial volume of water is at the sides of the cluster, and at the crevices and "outside" pores. For larger separations, but still within the class of loose clusters, the pattern of meniscus-type entries is similar. All AE are of meniscus instability mode. Interestingly, the first entry is almost invariably through the largest separation gap. Remembering that horizontal row top gap is 0.3 mm wide, while the bottom one is 0.5 mm, indeed, the AE for 0.1 mm separation is through 0.5 mm bottom gap, for 0.3 mm separation, through the right side 0.48 mm gap, for 0.6 mm separation through the left side 0.74 mm gap, while for 1mm separations, through the left side 1.05 mm gap. Timewise, AE occurs at 1870, 1540, 990 and 550 seconds into the process of evaporation, Fig. 7. The critical CS values at the first entry decrease with the separation and correspondingly are (see Hueckel et al., 2020): 0.28, 0.31, 0.54 and 0.75mm, meaning that the loosest assembly has the earliest initial AE.

Further instabilities take place at subsequent largest (in most cases) separations between adjacent grains, with the timing spaced relatively regularly. That means that air entry follows an opportunistic pattern of largest gaps between the grains, rather than formation of a consistent drying front. However, this may be rather a question of a scale of these observations, and of the size and form of the clusters tested. Indeed, it is at a larger scale, such as that modeled in Hale-Shaw apparatuses, that the sequence of the air-entries forms a high saturation gradient "drying front", tens to hundred grain diameters thick (see e.g. Armstrong et al., 2015). Not in one case of the considered batch the mode of the instability would become that of the double bowl.

For tight clusters, with zero horizontal gaps between the grains (within the rows, and with a half of the initial water volume, compared to the loose systems) the water body morphology evolution, Fig. 5, presents two features in common with the loose systems. First, the process consists in a slow motion of the external boundary at the rate of evaporation, followed by an abrupt, fast and substantial, but localized alteration of the boundary, and followed again by a slow motion of the boundaries, until the next instability develops. Second, the sequence of instabilities appears to be sensitive to random imperfections in the symmetry of the system. However, the initial instability for the tight systems has a completely different mechanism, as well as location, from that in loose clusters, and it occurs at one of two points with a double bowl-type (positive GC = both convex) curvature. Notably, as the grains are fixed we neglect all possible changes in horizontal solid-solid contact forces, as well as horizontal components of adhesive forces.

For the separation between the rows of 0.1 mm and 0.3mm the first instability occurs after a similar time elapse as for loose systems, about 30 min. for 0.1mm and 26min for 0.3mm through a thinning of water body from the front and back, at the central point of the pore. As the thickness of the water body decreases with the evaporation, it causes the front and the back surfaces to approach, forming effectively a thin-sheet at the point of local symmetry. The thin-sheet

then develops an instability in the form of a circular hole, which expands into a curvilinear triangle, and then stabilizes. This form of instability of a thin-sheet is well known in thin-sheet fluids (see Taylor and Michael, 1973, Anderson et al., 2010). For this central point of the pore, the diameter of an inscribed circle between the grains at the equatorial level is 0.363 mm (or 0.38mm), which effectively is the largest inter-grain gap of the system.

For the largest separation in tight systems, 0.5 mm, the instability mode takes place in 12 minutes and is at the saddle-form meniscus point. In fact, the side gap for that separation is quite large. The tight systems, compared to loose ones, except for D= 0.5mm, develop their first instabilities (air entry) at more advanced desaturation values.

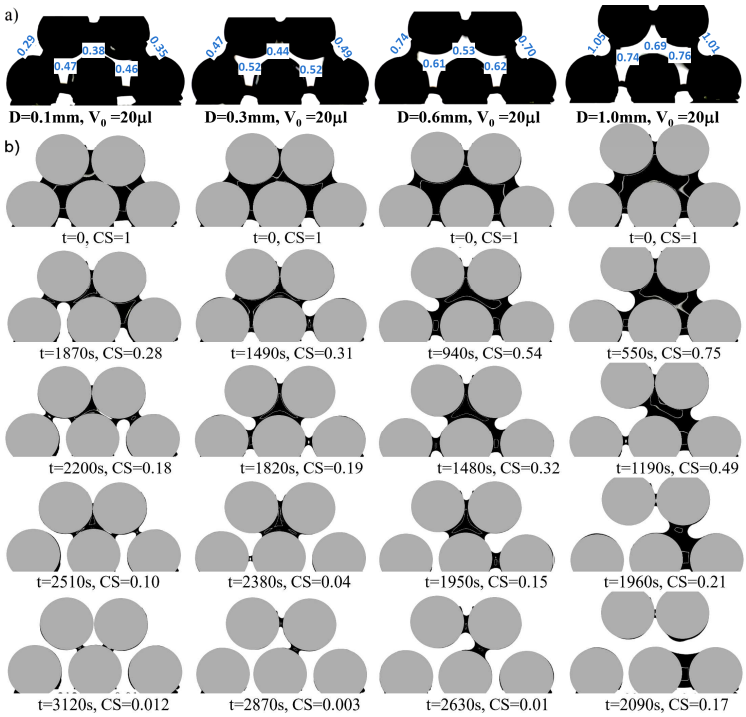

Fig. 5. Tight (no horizontal separation) cluster five-grain capillary water transitioning through capillary, funicular and pendular configurations: (a) separations between individual grains, see the caption for Fig. 4; (b) changes in in capillary water configuration for different separations D = 0.1mm, 1st column; of 0.3mm, second column; 0.5mm, third column.

Interestingly, for the two smallest separations in tight systems, 0.1 mm and 0.3 mm, after an initial double bowl instability, the subsequent instability mode is that of a saddle meniscus instability, followed again with a double bowl instability at the remaining pore location. In view of the evolution of the large system of 5 grains into 3- and 2- grain sub-systems, it is interesting to see that the evolution of such smaller but isolated systems follows the same patterns, as shown in an example of 3-grain system in a tight cluster evolving into a 3 pendular bridge configuration trough double-

bowl instability and loose arrangement evolving into two pendular bridges via a saddle-form meniscus instability, as shown in Fig.6 a and b, respectively.

At all larger separations in loose clusters the patterns are similar, but not identical.

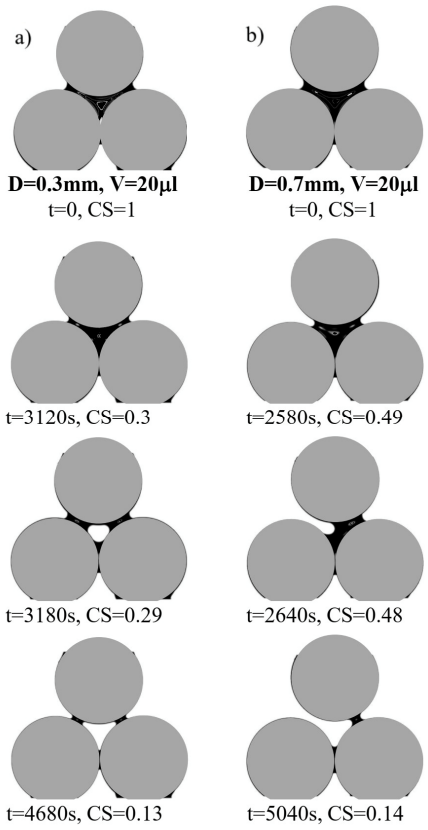

Fig. 6. Three-grain (8 mm) capillary water bridge evolution: (a) tight cluster) transitioning to three pendular configurations via double bowl instability; (b) loose cluster transitioning to two pendular configurations via saddle-form meniscus instability;

Hence, it is clear that more geometrically constrained (tight) systems tend to offer a larger variety of the instability modes.

2.2. Dynamic characteristics of capillary adhesion

In parallel to image collection, the tests on 5- grain clusters included the measurements of the intergranular capillary adhesion force between the two top row grains and the three bottom row grains, as it evolves during drying of the capillary bridge between them. These results were presented by Hueckel et al., 2020, and are reproduced here in Fig.7 plotted vs time of evaporation. This force is considered as a representation of the system one-dimensional adhesion

(Gibbs, 1906, Lian et al., 1991, Jain and Juanes, 2009, Hueckel et al., 2020). The non-dimensional force F_{CAP}* is used in order to compare the results obtained for different grain diameters. This force is expressed as

$$F_{CAP}^{*}=F_{CAP}/\gamma R \tag{1}$$

where γ is surface tension coefficient (0.072N/m) and R is radius of grain.

The results in Fig. 7, indicate a substantial similarity to the capillary force evolution for two-grain systems (Mielniczuk et al., 2015) and three- and four-grain systems (Hueckel et al., 2020). The force at the initial state varies between 0.3 to 0.6 x 10^{-3} N, very close indeed to the values for the 2-grain pendular systems (Hueckel et al., 2013). The maximum force value developed during evaporation, and hence the cluster adhesion depends on separation: the larger the separation, the lower and earlier the maximum value. The force exhibits between 30% to 300% increase of the initial attractive capillary force to a maximum of 1.13 x 10^{-3} N for the tightest cluster, followed by a decrease to zero of the force at the cluster saturation approaching zero.

During evaporation, the decreasing adhesion force reveals a series of up to three discontinuities, each of about 1/4th of the maximum force value. The occurrence of the force discontinuities coincides with the air entry events, that is gas/liquid interface instability events the morphology of which has been addressed earlier. No jump occurs during the increasing adhesive force stage of the process.

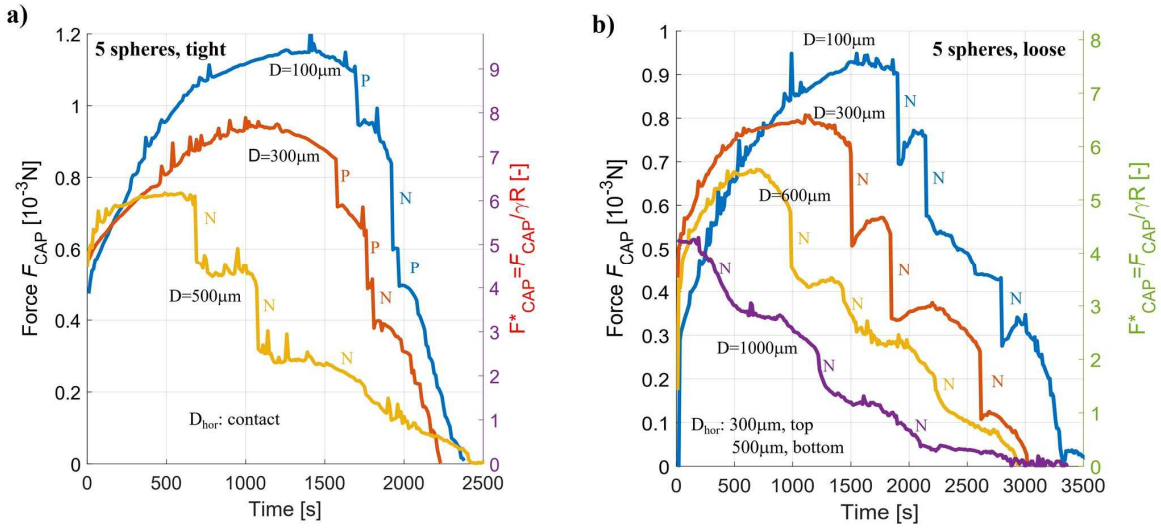

Fig. 7. Resultant capillary force evolution between the top and the bottom rows of grains (3.5 mm) in 5 – grain clusters as a function of time for different grain separations: (a) tight clusters; (b) loose clusters. N = negative, P = positive, Gaussian curvature point instability

The discontinuities occur for both loose systems (via meniscus instability mechanism (negative GC)), and for tight systems (at smaller separations 100 and 300 µm, via thin sheet instability (positive GC), whereas at larger separations, 1000µm, the instabilities take place via meniscus instability. Especially for the loose systems, there is a slight rebound of the force after the drop.

The resultant intergranular adhesion force for 3- and 4- grain systems, obtained by Hueckel et al., 2020, show a similar pattern to those for the 5-grain system. The instabilities of pendular (2-grain) bridges, which develop in the terminal phase of the evaporation of larger clusters were broadly addressed by Gagneux and Millet (2014) and Mielniczuk et al., (2015).

3. Capillary adhesion force and energy release at the air entries

The value of adhesion force at the air entry is particularly important as the first air entry is considered as a trigger of the macro-scale drying-crack onset (Scherer, 1992, Peron et al., 2009, Jain and Juanes, 2009, Hueckel et al., 2014). As argued before (Gibbs, 1906, see also Hueckel et al., 2020), at least at the micro-scale, the grains of clusters partially submerged in water are attracted via water bridges by two kind of forces: a resultant of water pressure (most often negative) acting during evaporation across a diminishing solid/liquid interface area and a resultant surface tension force acting along a decreasing solid/liquid/air contact line length. The orders of magnitude of the two resultants that were measured experimentally for two grain bridges, are very close, but their evolution trends are different. Similar conclusions were reached based on the Molecular Dynamics simulations for nano-scale capillary bridges (between two flat solid plates) by Fernandez-Toledano et al., 2017. It was therefore concluded (Hueckel et al., 2020), that rather than considering the evolution of an average capillary pressure (suction) as a sole variable controlling the cohesion as in phenomenological unsaturated porous media mechanics (see e.g. Bear, 1972, Fredlund et al. 1978, van Genuchten, 1980, Lu and Likos, 2004), it is more comprehensive to use the total intergranular capillary force per unit area, or adhesion, as a variable controlling the cohesion of the evaporating medium at a meso-scale, and reaching critical values at the moment of the first and subsequent air entries.

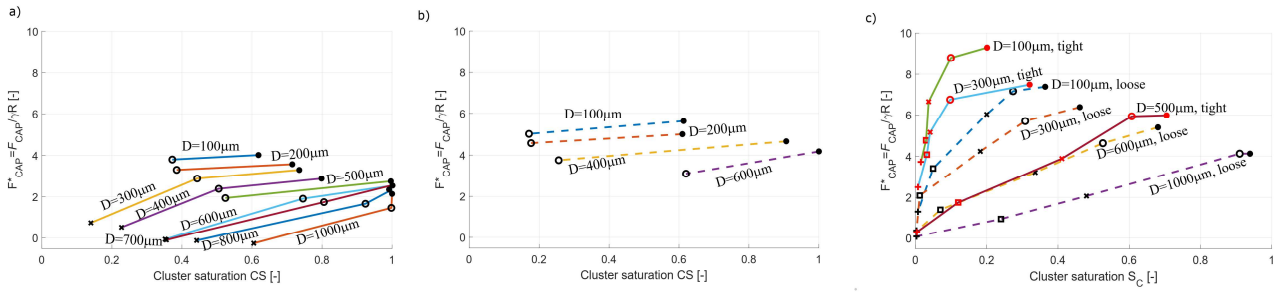

Fig. 8. The value of (non-dimensional) intergranular (adhesion) force $F_{CAP}^{*} = F_{CAP}/\gamma R$ at the onset of first (o), second (x), third (square) and fourth (+), consecutive jump (snap through) at the air entry for multi-grain clusters,; the force maximum is shown for comparison (full circles). (a) 3 grain cluster, (b) 4 grain cluster. (c) 5 grain clusters: loose (dashed line) and tight (solid line); Data for 3 & 4 grain clusters from Hueckel et al., 2020.

In what follows, the total intergranular capillary adhesion force value per entire cluster at an air entry moment is shown (Fig. 8) for a succession of entry events presented against cluster saturation, together with the force maximum value for reference (full dot), for 5- grain clusters, both tight and loose, as well as for 3- and 4- grain clusters. The data for the latter two cases are from Hueckel et al., 2020.

The first instability and the air entry for 5-grain clusters occur relatively soon after the capillary adhesive force reaches maximum, and at the corresponding force value is only slightly below (~5%) its maximum. For both tight, but also loose systems for small separations (lower porosity systems) the air entry is associated with higher intergranular forces, and it takes place when relatively lot of the initial water has evaporated. The larger the gap between the grains, the lower the intergranular force at the air entry and the smaller the amount fraction of water that has evaporated at the air entry.

For larger separations (loose clusters) simulating higher porosity media, the first instability and air entry occurs after between only 9% to 32% of water has evaporated from the cluster. For the smallest separations (tight clusters) the first air entry takes place after already 40-90% water has evaporated. This means that for loose soils the air would start to penetrate soil (and possibly crack it) so much earlier in the process than for the tight ones. As the media considered here are not deformable, that signifies that for loose systems the mechanism of desaturation through instabilities (air entry) kicks in much earlier than for the tight systems. For the tight systems, the water loss occurs mainly via slow surface evaporation over a large part of duration of the process, without much of instabilities until very late.

4. Discussion

It has to be underlined that in real soils that are deformable, the slow, external-surface evaporation stage of drying is accompanied by the shrinkage of the solid skeleton It is commonly assumed that the mechanism of that shrinkage is through suction transmitted to the pore system via water being drawn to the surface by a fraction of the evaporation flux (see e.g. Hu et al., 2013a). Meso-scale parametric simulations, both experimental and numerical (Hu et al., 2013b, and c, Bista et al.,2014) suggest that once gas enters the pore system it displaces liquid water much faster than during evaporation alone. It appears that the micro-scale experiments confirm that finding, even in a non-deformable system.

It is interesting to note that for tight clusters after the first (thin-sheet) instability, the systems evolve into a symmetric configuration, reduced to two parallel 3-grain sub-clusters and one horizontally connected 2-grain bridge for both 0.1mm and 0.3 mm separations. As shown by Hueckel et al., 2020, the isolated three-grain clusters exhibit qualitatively the same patterns as three-grain sub-clusters of the five-grain systems discussed above. Further developments of such sub-systems are the same as isolated 3-grain clusters. For both 3- grain sub-clusters, with a newly

formed saddle-form side-wise meniscus, an instability occurs, spilling eventually to the neighboring positive GC point. Immediately after, an independent and not- connected thin-sheet instability forms at the remaining positive GC point, for both 0.1 and 0.3 mm. Notably, the cluster saturations are quite low in both instances for the entire cluster, but clearly not if one considers the sub-clusters alone. Loss of the body of liquid water eventually leads to formation of a system of pendular bridges between pairs of grains, which finally rupture one after another, after ultimately evaporating a substantial fraction of their starting mass of water and degenerating into a water-wire, as described by Hueckel et al., 2013, Mielniczuk et al., 2015 and Yang et al., 2018. The remaining (often called residual) water forms stress-free water films around the pair-forming grains which eventually evaporate without further affecting stress transmission in the system.

One needs to address at this point the fact that since early on, one observes masses of water, often significant, that become isolated from the others, and hence not subject to any pressure gradient flows, and if evaporation conditions stop, behave as an inert water mass, and in analogy to strongly adsorbed water in clays effectively becomes a part of the solid skeleton (see Ma and Hueckel, 1992a, 1992b, Hueckel, 1992). These isolated masses of water, while subject to capillary forces, do not participate in any internal (or external) force transition chain. In the context of meso- and macro- scale media it appears more appropriate to refer to total (resultant) intergranular forces acting between the grains across a nominal surface area of a cluster, rather than to pressure (suction) in water bodies as a means to transfer the loads, as they may become separated in the process of drying.

In addition, the resultant forces from capillary pressure are not the only intergranular forces that produce adhesion within a capillary cluster. Forces of surface tension acting along the triple line of contact of all three phases are of the same order, but a distinctly different kinematics and direction. In what follows we discuss the force of adhesion at the onset of subsequent instability.

The focus in unsaturated soil mechanics is on the air entry understood as “the first air entry”, which is considered as equivalent to the onset of desaturation, and attributed with the corresponding pressure as an “air entry pressure”, as a property of a given soil. However, as the evaporation continues, the water/air interface evolves, subsequent instabilities and air entries (Haines jumps) take place at values of the intergranular adhesive force each time smaller, see Figs. 8 and 9, where data both for tight and loose clusters are shown. The observed adhesion force decrease is consistent with other cases (two-grain bridges (Mielniczuk et al., 2014a, 2015), with the intergranular force invariably decreasing to zero). The biggest values of adhesive force at corresponding subsequent jumps are at the smallest separations.

Each air entry is simultaneous with an intergranular adhesion force drop, roughly over the same order of the magnitude of about 2×10^{-4} N, which is about 20% of the maximum force for the loose systems, and about 12.5% for

the tighter systems (see Fig. 6). Interestingly, the amount of the drop is practically the same for both modes of air entry: the saddle-form meniscus instability and a thin-sheet (double bowl) instability, at similar separations.

Figure 9 shows that the value of the capillary adhesion force at the first air entry for a 5-grain cluster results to be smaller when the separations between grains are smaller, for both tight and loose clusters. The same is seen for subsequent jumps and for comparison for the maximum adhesion force generated in the drying process. A similar conclusion may be reached for the adhesion force at the air entries for smaller clusters of 3 and 4 grains presented above.

Both graphs suggest that for materials with lower porosity their onset of desaturation with an air entry would occur at a higher adhesion force. In other terms, "the drying cracking strength" is higher in lower porosity assemblies.

As the adhesive strength comes exclusively from the capillary bridges and their capillary pressure and surface tension force constituents and the first instability produces and hence is quasi simultaneous with a macro-scale drying crack onset, it is not surprising that it is smaller and smaller as the separations increase.

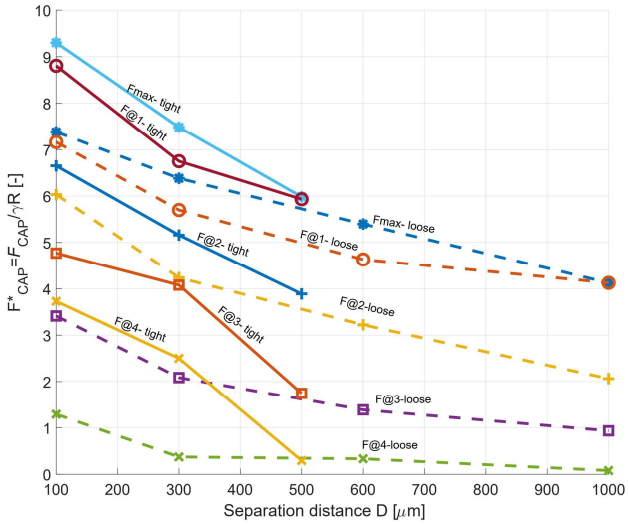

Fig. 9. The value of (non-dimensional) capillary adhesion force at the onset of the first, $F_{@1,}$ up to the fourth jump, $F_{@4}$ at the air entry for five-grain clusters, for different separations between grains: loose (solid-) and tight (dashed-line) clusters. Maximum adhesion force (F_{max}) is also shown for comparison (*).

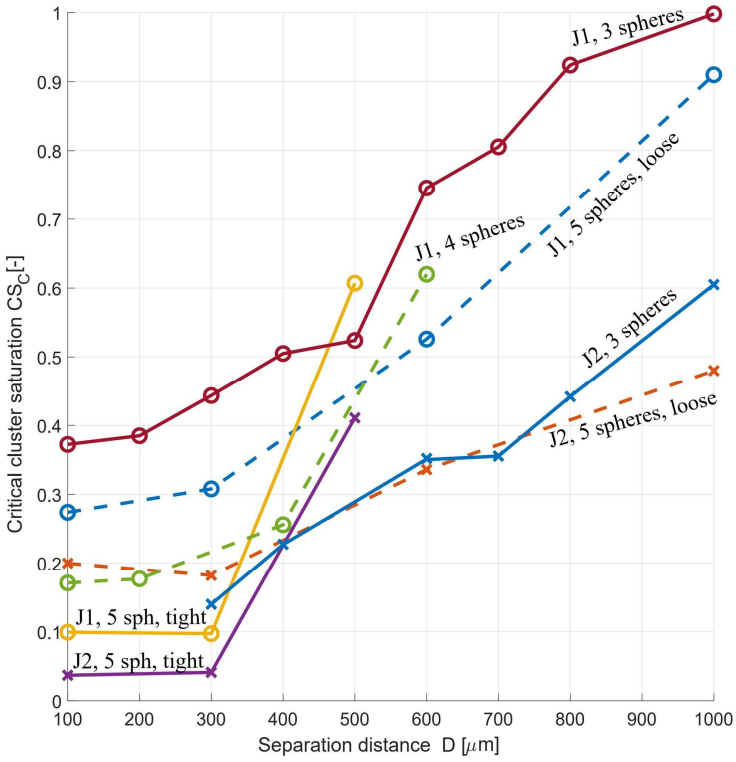

Fig. 10. The value of a critical cluster saturation at the onset of the first adhesion force jump, J1 (o) at the first air entry, and at the second force jump, J2 (x), for 3-, 4- and 5-grain clusters, for different separations between the grains

From the modeling point of view, and to build our intuition, it is useful to know what is the critical cluster saturation at which the air entry will take place. As shown in Fig. 10, the higher the separation between the grains (hence, the more porous the soil), the higher the critical saturation, or the wetter the soil, at which in the process of drying a given cluster will undergo the first air entry, and hence will potentially crack, if constrained, following the observation of Hueckel et al., 2014.

In the context of the above, from the data shown in Fig. 7 it is possible to identify the energy associated with the two equilibrium configurations, i.e. at the initial and the terminal instances of the instabilities. The difference between the two can be construed as the amount of energy released during the Haines jump (see also Cueto-Fulgueroso and Juanes, 2016). Notably, in the real systems the energy released is likely to be consumed in two modes: the dynamic motion of water mass and the deformation and possibly fracture of the granular skeleton (Holtzman and Juanes et al., 2010). In our experiments the grains are immobilized. Hence, the latter mode is impossible, and the total energy released goes to water.

Here, the adhesion energy release has been determined for the 5-grain systems at different separations. The energy may be expressed in several ways. Here it is defined as a measure of the energy release of the capillary adhesion force, F_{CAP} jump: through the difference of adhesion energy between the points of the onset and the end of the dynamic portion of the process: $I_a^{(1)}$- $I_a^{(2)}$, where adhesion energy is expressed as

$$I_a = -\int_0^{t_j} [F_{CAP}/A \cdot (\partial V_w/\partial t)]dt \quad (2)$$

appropriately per measured (horizontal) cross section surface area of the cluster, A, over the time interval from 0 to the time of jump, t_j, see Fig. 10a. V_w is the current capillary water volume. In this sense, the energy released comes from the change of both in capillary pressure force and in surface tension force components, jointly multiplied by the desaturation rate (which, may be argued is an arbitrarily chosen measure). The energies released during the jumps are plotted in Fig. 10b and c, for loose and tight clusters respectively, as a function of Cluster Desaturation degree, 1- CS. It is to be noted that the adhesion energy chosen here does not correspond to that of L/S surface energy for the flat interface without capillary pressure effect. Given that we have an adhesion composed of two independent forces acting respectively on a volume and a length changes, we chose an energy measure (that can be seen as an arbitrary choice), but nevertheless representing the trend (decreasing) of the jump impact.

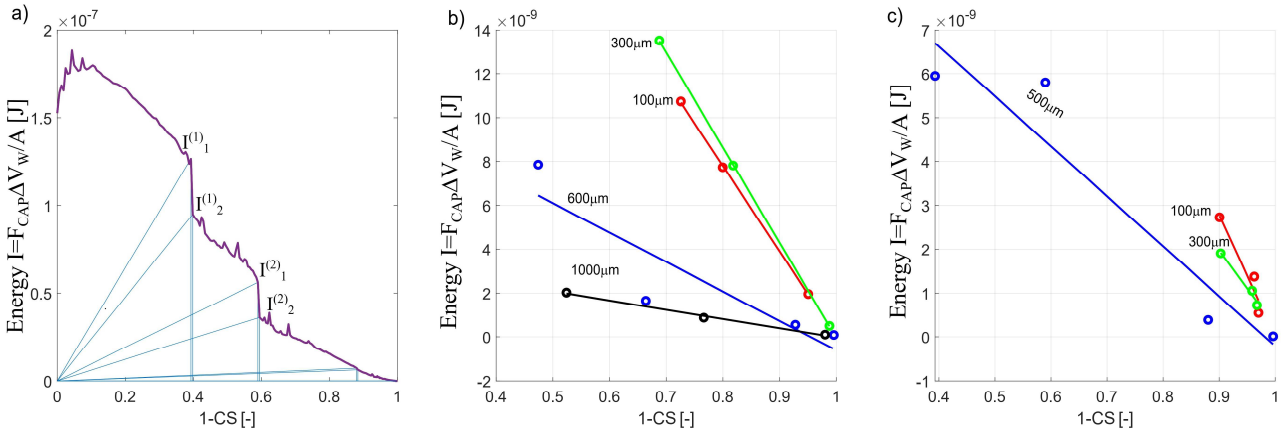

Fig. 11a) Assessment of energy released during subsequent air entry instabilities, an example for a tight 5-grain cluster at a grain separation 500um; 10b) Energy release during subsequent Haines jumps vs desaturation degree, 1-S_c for different separations for loose clusters, 10 c) Energy release during subsequent Haines jumps vs desaturation degree, 1-S_c for different separations for tight clusters.

It is seen that the energy release during Haines jumps heavily depends on the separation within the cluster (decreasing with it), even stronger than the adhesive forces at the jumps depend on it. For the largest separation of 1000 um, for loose clusters, the first air entry involves almost one order of magnitude less energy released than for the smallest separation. The final jumps carry a minimal energy, given a low level of adhesion. The released energy is decreasing for the subsequent jumps, both for loose and tight clusters. Clearly, at each subsequent jump there is visibly less water to be moved. So, as the process advances, the role of the jumps diminishes in propelling the air/water interface in comparison to the evaporation mechanism.

5 Concluding remarks

Air entry is an extremely important phenomenon in desiccation process of soils, for at least two reasons: it marks the onset of macro-scale desaturation and it creates conditions for drying-cracking at micro-scale. Especially drying-cracking is of a great practical importance, as it is linked to diverse forms of damage of geo-structures. While both events are classically referred to macro-scale occurrences, their origins are traced to micro-scale conditions. Understanding mechanisms and their correlations to principal variables of the phenomena involved on the models such as idealized few grain clusters considered here contributes to a better understanding and control of the actual phenomena at the field scale.

The above findings offer an alternative perspective on the interpretations of the air entry. First, the concept of the air entry pressure as an independent and its sole criterion (marker) calls for reevaluation, as it clearly ignores the role of the surface tension force in the air entry instability event (as discussed already by Gibbs, 1906, see also Hueckel et al., 2014, 2020). Second, the experiments clearly show a repetition of the unstable snap-throughs, progressively at a lower value of the capillary adhesion force, and at a lower associated saturation.

In general, the three modes of evolution of water configuration mentioned earlier, determine the mode of air entry into the water body. The air entry mode is different for positive (double bowl), negative (or saddle-form meniscus) and zero (flat, at least in one cross-section) Gaussian curvature (GC) points. GC is the product of the two principal curvatures, of the water body surface.

With the techniques currently available, we are not able to measure the two principal curvatures at the same time, and hence to calculate a value for the capillary pressure. Neither we are in the position to do that for the GC, nor to advance a hypothesis about quantitative criteria for the air entry in generic configuration.

Thus a critical adhesion force at the first air entry, or a critical adhesion per unit area is offered as a phenomenological threshold of strength of soil against drying-cracking. It is yet to be proven experimentally for a wider data base.

It is concluded from the foregoing observation that the higher the separation between the grains or in general, the higher the soil porosity, the higher the critical cluster saturation, i.e. the wetter the soil, at which first air entry and hence drying-cracking will occur, if constrained. At the same time, the higher the separation between the grains or in general, the higher the soil porosity, the higher the critical adhesion, or strength against drying cracking.

The first air entry episode appears to take place through the largest available gorge over the perimeter of the cluster, confirming the previous findings. The progress of the subsequent air entries seems to follow the same criterion: through the largest available gorge of the current interface, rather than forming a drying front, or a directed crack. That however

is the question of the scale of the models used. To detect the latter modes a meso-scale experiment (Hale-Shaw apparatus test) appears to be appropriate.

Subsequent air entries into saturated regions of the medium, occurring at a progressively lower saturation take place at a lower and lower critical adhesion force. Consequently, the energy released during the subsequent Haines jumps is progressively lower.

Needless to say, the above conclusions are valid for the small regular clusters, and to validate them for the actual soil continua, an upscaling sequence of procedures needs to be applied.

Finally, previous findings suggesting the air entry as a precursor to the onset of drying-cracking (Peron et al., 2009a, b, Jain and Juanes, 2009, Holtzman and Juanes, 2010, Hueckel et al., 2014) need to be confirmed for a wider data base.

The authors (B.M. & T.H.) acknowledge the support of US DOE grant DE-NE0008746.

References

Alonso, E. E., Pereira, J. M., Vaunat, J. & Olivella, S. (2010). A microstructurally based effective stress for unsaturated soils. Géotechnique 60, No. 12, 913–925, https://doi.org/10.1680/geot.8.P.002.

Anderson, A. M., Brush, L. N., Davis, S. H., 2010. Foam mechanics: spontaneous rupture of thinning liquid films with Plateau borders. Journal of fluid Mechanics, 658, 63-88. https://doi.org/10.1017/S0022112010001527

Armstrong, R.T., Evseev, N., Koroteev, D., Berg, S., 2015. Modeling the velocity field during Haines jumps in porous media. Adv. Wat. Resour. 77, 57–68. https://doi.org/10.1016/j.advwatres.2015.01.008.

Bear, J., 1972. Dynamics of Fluids in Porous Media. Elsevier, New York.

Bista, H Hu, LB, Mielniczuk, B., El Youssoufi, M. S., Laloui, L., Hueckel, T., 2014. Multi-scale study of desiccation shrinkage in granular soils. Unsaturated Soils: Research & Applications, vols. 1 and 2, CRC Press, London, Edited by:Khalili, N; Russell, AR; Khoshghalb, A, 883-889

Cueto-Felgueroso, L., Juanes, R., 2016. A discrete-domain description of multiphase flow in porous media: Rugged energy landscapes and the origin of hysteresis. Geophys. Res. Lett., 43, 1615–1622, https://doi.org/10.1002/2015GL067015.

Fernandez-Toledano, J.C., Blake, T.D., Lambert, P., De Coninck, J., 2017. On the cohesion of fluids and their adhesion to solids: Young's equation at the atomic scale. Adv. Colloid Interface Sci. 245, 102-107. https://doi.org/10.1016/j.cis.2017.03.006.

Fredlund, D. G., Morgenstem, N. R., Widger, R. S., 1978. The shear strength of unsaturated soils. Can. Geotech. J. 15, 313-321. https://doi.org/10.1139/t78-029.

Fisher, R. A., On the capillarity forces in an ideal soil; correction of formulae given by W. B. Haines, J. Agric. Sci. 16 (1926) 492–505

Gagneux, G., Millet, O. (2014), Analytic calculation of capillary bridges properties deduced as an inverse problem from experimental data. Transport in Porous Media 105, 117–139.

van Genuchten, M.T., 1980, A closedform equation for predicting the hydraulic conductivity of unsaturated soils. Soil Sci. Soc. Am. J., 44, 892-898. https://doi.org/10.2136/sssaj1980.03615995004400050002x.

Gibbs, J.W., 1906, The Scientific Papers, vol 1. Thermodynamics, Longmans, Green, and Co, London, 1906.

Gras, J. P. (2011). Approche micromécanique de la capillarité dans les milieux granulaires: rétention d'eau et comportement mécanique., PhD thesis, Université Montpellier 2, Montpellier, France.

Gras, J. P., Delenne, J. Y. & El Youssoufi, M. S. (2013). Study of capillary interaction between two grains: a new experimental device with suction control. Granular Matter 15, No. 1, 49–56.

Guo, R., Hueckel, T. 2013. Growth of polymer microstructures between stressed silica grains: a chemo-mechanical coupling, Ge´otechnique 63, 4, 322–330 http://dx.doi.org/10.1680/geot.SIP13.P.021

Guo, R., Hueckel, T., 2015. Silica polymer bonding of stressed silica grains: An early growth of intergranular tensile strength. Geomechanics for Energy and the Environment 1, 48-59, https://doi.org/10.1016/j.gete.2015.02.002

Haines,W. B. (1930). Studies in the physical properties of soil. V. The hysteresis effect in capillary properties, and the modes of moisture distribution associated therewith. J. Agric. Sci. 20, No. 1, 97–116.

Holtzman, R., Juanes, R., 2010. Crossover from fingering to fracturing in deformable disordered media. Phys. Rev. E 82, 4, 046305. https://doi.org/10.1103/PhysRevE.82.046305.

Hu, L.B., Péron, H, Hueckel, T., Laloui, L., 2013a. Desiccation shrinkage of non-clayey soils: multiphysics mechanisms and a microstructural model. Int. J. Numer. Anal. Meth. Geomech. 37, 12, 1761-1781, DOI:10.1002/nag.2108.

Hu, L.B., Péron, H, Hueckel, T., Laloui, L., 2013b. Desiccation shrinkage of non-clayey soils: a numerical study, Int. J. Numer. Anal. Meth. Geomech. 37, 12, 1782-1800, DOI: 10.1002/nag.2107.

Hu, LB, Peron, H Hueckel, T., Laloui, L., 2013c. Mechanisms and critical properties in drying shrinkage of soils: experimental and numerical parametric studies. Can. Geo. J. 50, 536-549. DOI: 10.1139/cgj-2012-0065.

Hueckel, T., 1992. Water - Mineral Interaction in Hygro-Mechanics of Clays Exposed to Environmental Loads: a Mixture Theory Approach. Can. Geo. J., 29, 1071-1086. https://doi.org/10.1139/t92-124.

Hueckel, T., Mielniczuk, B., El Youssoufi, M. S., 2013. Micro-scale study of rupture in desiccating granular media. In: C. Meehan et al. (eds.), Proc. Geo-Congress 2013 "Stability and Performance of Slopes and Embankments III", 3-7 March 2013, San Diego, USA, ASCE GSP No. 231, 808-817, https://doi.org/10.1061/9780784412787.082.

Hueckel, T., Mielniczuk, B., El Youssoufi, M.S., Hu, L. B., Laloui, L., 2014. A three-scale cracking criterion for drying soils. Acta Geophys. 62, 1049 https://doi.org/10.2478/s11600-014-0214-9.

Hueckel, T., Mielniczuk, B., El Youssoufi, M.S., 2020. Adhesion-force micro-scale study of desiccating granular material, Geotechnique, 70, 12. https://doi.org/10.1680/jgeot.18.p.298.

Jain, A. K., and R. Juanes (2009), Preferential Mode of gas invasion in sediments: Grain-scale mechanistic model of coupled multiphase fluid flow and sediment mechanics, J. Geophys. Res., 114, B08101, doi:10.1029/2008JB006002.

Lian, G., C. Thornton, and M. J. Adams, 1991, A theoretical study of the liquid bridge forces between two rigid spherical bodies, J. Colloid Interface Sci., 161, 138–147, doi:10.1006/jcis.1993.1452.

Lievano D., Velankar, S., McCarthy, J.J., 2017. The rupture force of liquid bridges in two and three particle systems. Powd. Tech. 313, 18-26, https://doi.org/10.1016/j.powtec.2017.02.053.

Lu, N., Likos, W.J., 2004. Unsaturated soil mechanics. John Wiley & Sons., Hoboken, NJ, USA.

Ma, C., Hueckel, T., 1992a. Stress and pore pressure in saturated clay subjected to heat from radioactive waste: a numerical simulation. Can. Geo. J. 29, 1087. https://doi.org/10.1139/t92-125.

Ma, C., Hueckel, T., 1992b. Effects of Inter-phase Mass Transfer in Heated Clays: a Mixture Theory. International Journal of Engineering Sciences, 30, 11, 1567-1582. https://doi.org/10.1016/0020-7225(92)90126-2.

Måløy, K. J., Furuberg, L., Feder, J. & Jøssang, T., 1992. Dynamics of slow drainage in porous media. Phys. Rev. Lett. 68, No. 14, 2161–2168.

Mielniczuk, B., Hueckel, T., El Youssoufi, M. S., 2014a. Evaporation-induced evolution of the capillary force between two grains. Granular Matter 16, 815-828. https://doi.org/10.1007/s10035-014-0512-6.

Mielniczuk, B., El Youssoufi, M. S., Sabatier, L., Hueckel, T., 2014b. Rupture of an evaporating liquid bridge between two grains. Acta Geophysica 62, 1087-1108, https://doi.org/10.2478/s11600-014-0225-6.

Mielniczuk, B., Hueckel, T., El Youssoufi, M. S., 2015. Laplace pressure evolution and four instabilities in evaporating two-grain liquid bridges. Powder Technol. 283, 137-151. https://doi.org/10.1016/j.powtec.2015.05.024.

Orr, F. M., Scriven, L. E., Rivas, A. P., 1975. Pendular rings between solids: Meniscus properties and capillary force, J. Fluid Mech., 67, 723 – 742, doi:10.1017/S0022112075000572.

Péron, H., Hueckel, T., Laloui, L., Hu, L.B, 2009. Fundamentals of desiccation cracking of fine-grained soils: experimental characterization and mechanisms identification. Can. Geotech. J. 46, 10, 1177-1201. https://doi.org/10.1139/T09-054.

Péron, H. , Laloui, L., Hueckel, T., Hu, L.B. (2009b), Desiccation cracking of soils, European Journal of Environmental and Civil Engineering, 13, 7-8, 869-888.

Scherer, G.W. 1992, Crack-tip stress in gels, *J. Non-Cryst. Solids* **144**, 210-216, DOI:10.1016/S0022-3093(05)80402-8.

Taylor, G. I., Michael, D. H., 1973. On making holes in a sheet of fluid. J. Fluid Mechanics 58, 625-639. https://doi.org/10.1017/S0022112073002375.

Urso, M.E., C. J. Lawrence, M. J. Adams, 1999, Pendular, Funicular, and Capillary Bridges: Results for Two Dimensions, Journal of Colloid and Interface Science 220, 42–56.

Yang, S., Hueckel, T., Mielniczuk, B., El-Youssoufi, M.S., 2018. A note on evolution of pressure and flow within evaporating capillary bridge. European Physics Journal, E (Soft Matter), 41, 140-149. https://doi.org/10.1140/epje/i2018-11748-x.

Zhao, Ch-F., Kruyt, N.P., Millet, O., 2020. Capillary bridges between spherical particles under suction control: Rupture distances and capillary forces. Powd. Tech. 360, 622-634. https://doi.org/10.1016/j.powtec.2019.09.093.